

Chemical Science

Accepted Manuscript

This article can be cited before page numbers have been issued, to do this please use: S. Ishihara, A. Ghosh, T. Mori, M. Chahal, D. T. Payne, A. Saeki, T. Hyakutake and T. Nakanishi, *Chem. Sci.*, 2026, DOI: 10.1039/D5SC08398B.



This is an Accepted Manuscript, which has been through the Royal Society of Chemistry peer review process and has been accepted for publication.

Accepted Manuscripts are published online shortly after acceptance, before technical editing, formatting and proof reading. Using this free service, authors can make their results available to the community, in citable form, before we publish the edited article. We will replace this Accepted Manuscript with the edited and formatted Advance Article as soon as it is available.

You can find more information about Accepted Manuscripts in the [Information for Authors](#).

Please note that technical editing may introduce minor changes to the text and/or graphics, which may alter content. The journal's standard [Terms & Conditions](#) and the [Ethical guidelines](#) still apply. In no event shall the Royal Society of Chemistry be held responsible for any errors or omissions in this Accepted Manuscript or any consequences arising from the use of any information it contains.

Luminescent core-isolated solvent-free liquids as a soft material platform for optical gas sensing

Shinsuke Ishihara,^{a,*†} Avijit Ghosh,^{a,b,†} Tatsuya Mori,^{a,‡} Mandeep K. Chahal,^{a,c} Daniel T. Payne,^{a,d} Akinori Saeki,^e Tsuyoshi Hyakutake,^f Takashi Nakanishi^{a,*}

^aResearch Center for Materials Nanoarchitectonics (MANA), National Institute for Materials Science (NIMS), 1-1 Namiki, Tsukuba, Ibaraki 305-0044, Japan

^bSchool of Natural and Applied Science, Department of Forensic Science & Technology, Maulana Abul Kalam Azad University of Technology, Haringhata 741249, West Bengal, India

^cSchool of Chemistry and Forensic Science, University of Kent, Canterbury, CT2 7NH, UK

^dSchool of Life, Health & Chemical Sciences, The Open University, Milton Keynes, MK7 6AA, UK

^eDepartment of Applied Chemistry, Graduate School of Engineering, Osaka University, 2-1 Yamadaoka, Suita, Osaka, 565-0871, Japan

^fInnovative Materials Resources Research Center, Public Works Research Institute, 1-6 Minamihara, Tsukuba, Ibaraki, 305-8516, Japan

[†]These authors contributed equally to this work

[‡]Present address: Department of Chemistry, Graduate School of Science and Integrated Research Consortium on Chemical Sciences (IRCCS), Nagoya University, Furo, Chikusa, Nagoya, 464-8602, Japan

*Correspondence: ISHIHARA.Shinsuke@nims.go.jp, NAKANISHI.Takashi@nims.go.jp

Keywords: functional liquids, porphyrins, phosphorescence, ratiometry, gas sensing

Abstract: Solvent-free functional molecular liquids have attracted great interest as a new class of stimuli-responsive soft materials, yet their potential as optical gas sensors remains unexplored. Conventionally, luminescent organic molecules are employed in combination with a solid support or matrix. However, their performance in chemical sensing and optoelectronic devices is often hindered by adverse phenomena such as aggregation, concentration quenching, and photodegradation. In this study, we employ a strategy to isolate and wrap a phosphorescent Pt(II)-porphyrin core with bulky yet flexible branched alkyl chains, resulting in a solvent-free liquid at room temperature that demonstrates excellent properties for sensing oxygen (O_2) gas. Compared to reference material composed of Pt(II)-tetraphenylporphyrin and a highly gas-permeable polymer matrix, our Pt(II)-porphyrin liquid shows comparable sensitivity ($I_0/I_{100} = 75\sim90$), better linearity, and greater photostability in its O_2 -responsive phosphorescence. This is attributed to the high homogeneity and gas solubility of the liquids, as well as to the shielding of luminescent-core units by bulky alkyl chains. The liquid nature of the materials allows for ratiometric sensing, where the compatibility of a phosphorescent Pt(II)-porphyrin liquid (O_2 -sensitive) and a fluorescent alkyl-pyrene liquid (O_2 -insensitive) enables reproducible monitoring of O_2 concentration without specific calibration. Indeed, these results highlight the significant benefits of core-isolated luminescent liquids in diverse sensing applications.



Introduction

Functional molecular liquids (FMLs) have recently become a transformative category in soft functional materials.¹ Within this group, alkyl- π liquids—solvent-free systems with π -conjugated molecular units isolated and wrapped by bulky yet flexible branched alkyl chains—provide tunable optoelectronic properties and liquid-phase behaviors that differ from traditional solid-state frameworks.^{2–4} These alkyl- π liquids have unique physical properties: molecular uniformity, fluidity, deformability, miscibility, and guest solubility, etc. Owing to their abundant designability for functional core units, various types of FMLs have been developed to date (e.g., tunable luminescence including phosphorescence,^{5–9} triplet-mediated photochemical functions,^{10,11} optoelectronic- and energy-related functions,^{12–14} permanent porosity and gas adsorption,^{15,16} and guest- and mechano-responsiveness^{17–21}). Among those intriguing FMLs, although alkyl- π liquids have been developed as stimuli-responsive liquid materials, to the best of our knowledge, no reports have demonstrated the utility of their liquid properties for optical gas sensing. In related works, Isoda et al. reported alkylated *N*-heteroacene liquids that change their fluorescence color upon exposure to HCl vapor, where the vapor responsiveness is accompanied by protonation-induced solidification of the liquids.^{20,21} Unique aspects of alkyl- π liquids include their ability to provide a distinct mode of operation as stable liquid media that retain responsiveness and miscibility. According to Henry's law, the dissolution of gas molecules into liquids is proportional to their partial pressure.²² This motivated us to elucidate the potential of alkyl- π luminescent liquids as optical gas sensors and unveil any fundamental aspects distinct from conventional solid support or matrix systems.

Luminescent organic molecules (LOMs) have been utilized for optical sensing of physical, chemical, and biological events.^{23–26} In particular, oxygen (O₂) is a vital target analyte^{27–29} due to strong connections with the atmospheric environment, energy, and life, as exemplified by the spatiotemporal visualization of aerodynamics,³⁰ fuel cell operation,³¹ and hypoxia in cancer cells.^{32,33} Among the various optical detection modes (e.g., wavelength, intensity, ratiometric, frequency, upconversion, lifetime, etc.), monitoring of luminescence intensity is widely utilized in O₂ sensing due to the low cost and simplicity of the devices.^{24,29} Triplet photo-excited states of LOMs can be effectively quenched by O₂, which makes their phosphorescence intensity sensitive to O₂ levels. The interaction dynamics and correlation between luminescence intensity and a quencher's concentration are described by the Stern-Volmer equation (eq. 1).²⁷



$$I_0/I_x - 1 = K_{sv}[Q] \quad (\text{eq. 1})$$

where I_0 and I_x are, respectively, the emission intensity in the absence (0%) and the presence ($x\%$) of a quencher (herein, O_2), and K_{SV} is the Stern-Volmer constant.

Since the luminescence of LOMs is generally maximized in their discrete (*i.e.*, non-aggregated) states except for rare cases where molecular motion is restricted within the aggregate or confinement,³⁴ optical sensing is often performed in a solution (dissolved in water or organic solvent) or a composite with solid support or matrix (*e.g.*, polymers,^{35–37} oxides,^{38,39} porous materials,^{40–42} and nanoparticles^{43–45}). Consequently, the performance of optical O_2 sensors is influenced not only by LOMs but also by the compatibility and O_2 permeability of the solid support or matrix. Among various phosphorophores (*e.g.*, polycyclic aromatic carbons, transition metal complexes, and fullerenes), Pt(II) and Pd(II)-porphyrins are extensively studied for optical O_2 sensing because of their intense phosphorescence at room temperature.^{27,46–48} For example, Amao et al. found that Pt(II)-octaethylporphyrin (**PtOEP**) embedded in a highly gas-permeable poly(1-trimethylsilyl-1-propyne) (**PTMSP**)⁴⁹ shows considerable sensitivity to O_2 ($I_0/I_{100} = 225$). In contrast, the same Pt(II)-porphyrin embedded in polystyrene or poly(dimethylsiloxane) exhibits only moderate sensitivity ($I_0/I_{100} = \sim 5$).⁵⁰

Here, we present the first demonstration of an optical oxygen (O_2) sensing based on a phosphorescent core-isolated solvent-free liquid, utilizing a Pt(II)-porphyrin core ([5,10,15,20-tetrakis(3,5-bis((2-hexyldecyl)oxy)phenyl)porphyrinato]platinum(II) **PtPL**, **Figure 1**). The liquid exhibits benchmark-level sensitivity ($I_0/I_{100} = 75\sim90$), superior linearity, and improved photostability compared to conventional reference materials composed of Pt(II)-tetraphenylporphyrin (**PtTPP**)⁵¹ and **PTMSP**. Additionally, by mixing **PtPL** with a fluorescent alkyl-pyrene liquid, we develop a robust ratiometric sensing that operates without specific calibration. This work provides novel insights into optical gas sensing, establishing luminescent solvent-free liquids not only as responsive FMLs but also as active media, opening a versatile pathway toward a future soft sensing platform.



Results and Discussion

To obtain Pt(II)-porphyrin liquid **PtPL**, a free-base liquid porphyrin with 2-hexyldecyl branched alkyl chains¹³ was reacted with Pt(II)Cl₂ in refluxing benzonitrile for 4-5 h under argon (Ar) (**Figure 1a**).⁵¹ After drying under vacuum, **PtPL** was obtained as a viscous red-orange liquid (**Figure 1b**). Disappearance of the inner pyrrolic protons in the ¹H NMR spectrum of **1** indicates the successful insertion of a Pt(II) ion into the porphyrin core, and the high-resolution mass spectrum of **PtPL** is in agreement with its chemical formula, [C₁₇₂H₂₈₅O₈N₄¹⁹⁴Pt]⁺ (**Figure S2-S5**). Under ultraviolet (UV) irradiation, an intense red emission was observed from **PtPL** when under an N₂ or Ar atmosphere (**Figure 1c**). The emission was largely quenched in air due to energy transfer from photo-excited **PtPL** to O₂. Thus, **PtPL** exhibits the expected phosphorescent properties for a long-lived triplet excited state. Even though branched alkyl chains surround the Pt(II) porphyrin core, small gas molecules can access the core through a mechanism akin to the facilitation of pyridine vapor into Zn(II) liquid porphyrin,¹³ which is structurally similar to **PtPL** (see **Figures S6-9, 21**).

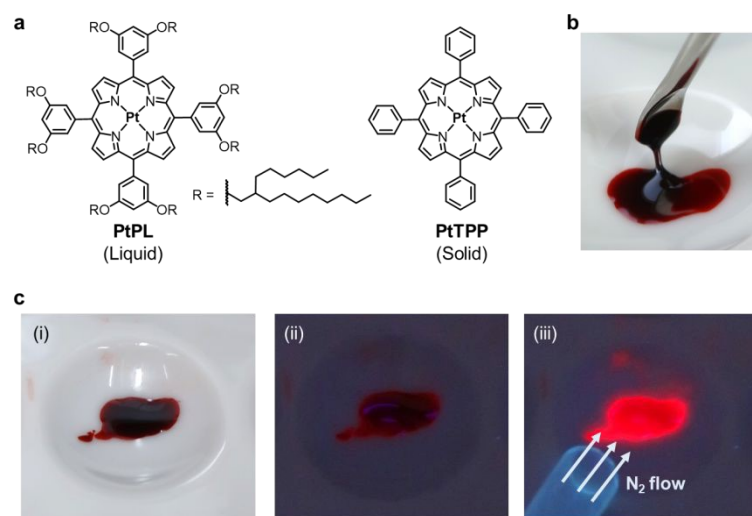


Figure 1. (a) Chemical structures of Pt(II) porphyrins; alkylated liquid (**PtPL**) and solid **PtTPP** used in this study. (b) Photograph of **PtPL** at 20 °C showing solvent-free liquid appearance. (c) Phosphorescent property of **PtPL** observed under daylight in air (i), under UV light in air (ii), and under UV light with N₂ flow (iii).

It is revealed that **PtPL** is a stable liquid at room temperature and shows optical properties in neat state almost identical to **PtTPP** in a diluted toluene solution (**Figure 2**). A sample of **PtPL** sandwiched between glass plates is fluidic, and its cross-polarized optical microscopy (POM) image shows no birefringence, supporting the absence of long-range ordered domains (**Figure 2a**). Differential scanning calorimetry (DSC) thermogram of **PtPL** shows only a reversible glass transition temperature (T_g) at around -40 $^{\circ}\text{C}$; thus, **PtPL** maintains a liquid state above that temperature (**Figure 2b**). Absorption and emission spectra of **PtPL** in neat liquid are similar to those of **PtPL** and **PtTPP** in toluene due to the bulky alkyl chains isolating the Pt(II)-porphyrin core from the surrounding environment (**Figures 2c and 2d**). Note that the luminescent lifetime and quantum yield of **PtPL** were slightly longer and larger than those of **PtTPP** in toluene (**Figure S11, Table S1**).

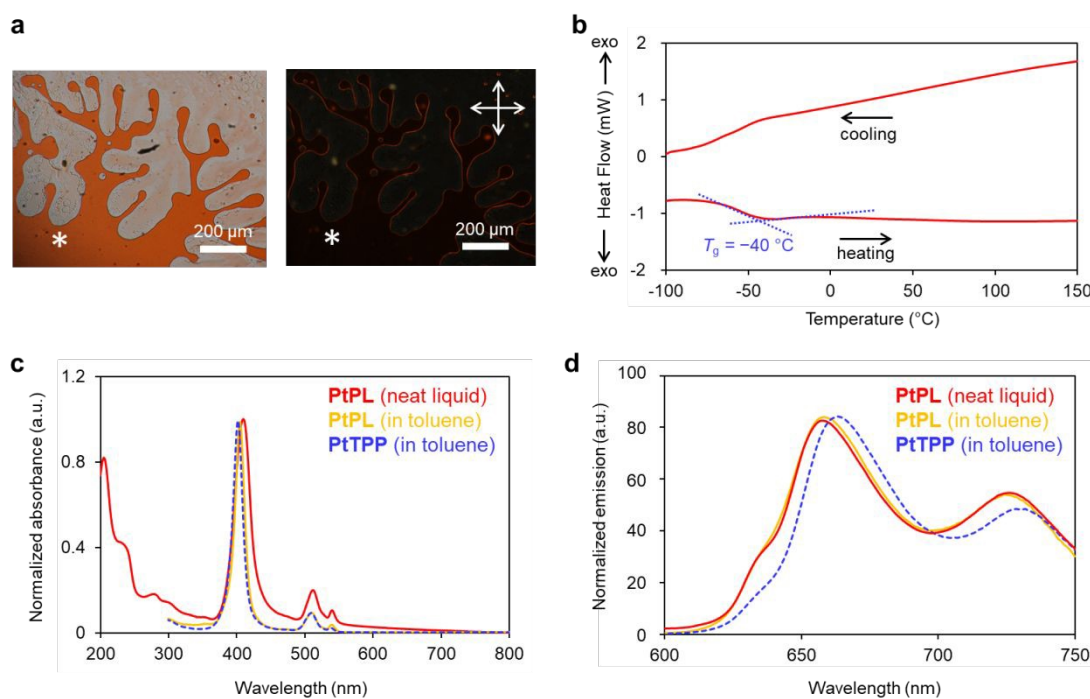


Figure 2. (a) Optical microscopy images of **PtPL** sandwiched between glass plates without (left) and with (right) cross polarizers. Asterisks (*) represent the identical positions within the samples. (b) DSC thermogram in the 2nd heating and cooling trace of **PtPL** recorded under N_2 at a scan rate of 10 $^{\circ}\text{C min}^{-1}$. (c) Absorption spectra of **PtPL** in neat liquid state. The absorption spectra of **PtPL** and **PtTPP** in toluene (10^{-6} M) are shown for comparison. (d) Emission spectra of **PtPL** in neat liquid state ($\lambda_{\text{ex}} = 410$ nm) under argon (Ar). The emission spectra of **PtPL** and **PtTPP** in toluene

(10^{-6} M) under Ar are shown for comparison. Note that these emissions were largely quenched under air (see **Figures S12-14**).

As shown in **Figure 3a-c**, the emission from neat film **PtPL** is quenched (signal intensity is reduced) as the concentration of O_2 in the atmosphere increases from 0% to 100%. There is a certain response to 0.03% O_2 , and the emission intensity halved at an O_2 concentration of 1% (**Figure 3a**). The Stern-Volmer plot of neat film **PtPL** shows linear correlations between O_2 concentration (x-axis) and $I_0/I_x - 1$ (y-axis). The value of I_0/I_{100} is often used in the literature to represent O_2 sensitivity, and $I_0/I_{100} = \sim 90$ is much greater than most phosphorescent O_2 sensing materials ($I_0/I_{100} = 5 \sim 10$).^{27,35,42} As described above, Amao et al. reported that **PtOEP** embedded in polystyrene or poly(dimethylsiloxane) shows modest sensitivity ($I_0/I_{100} = \sim 5$).⁵⁰ Whereas, significant sensitivity to O_2 ($I_0/I_{100} = 225$) was obtained when **PtOEP** was embedded in a highly gas-permeable **PTMSP** polymer. Thus, our solvent-free liquid **PtPL** is a suitable medium for accommodating O_2 molecules from the gas phase. The higher sensitivity of Amao's film could be ascribed to the excellent gas permeability of **PTMSP** as well as minimum substituents around the Pt(II)-porphyrin unit, enabling efficient energy transfer to proximal O_2 . However, it should be noted that the porphyrin concentration in the Amao's film was very dilute (ca. 2.9×10^{-5} mol dm⁻³, estimated as ca. 0.003 wt% based on molecular weight of the **PtOEP** (727.8 g mol⁻¹) and density of **PTMSP** (0.7 g cm⁻³)⁵²), presumably for preventing undesirable aggregation of porphyrins in the polymer matrix. Therefore, compared to the neat liquid **PtPL**, the brightness of the **PtOEP-PTMSP** film should be modest.



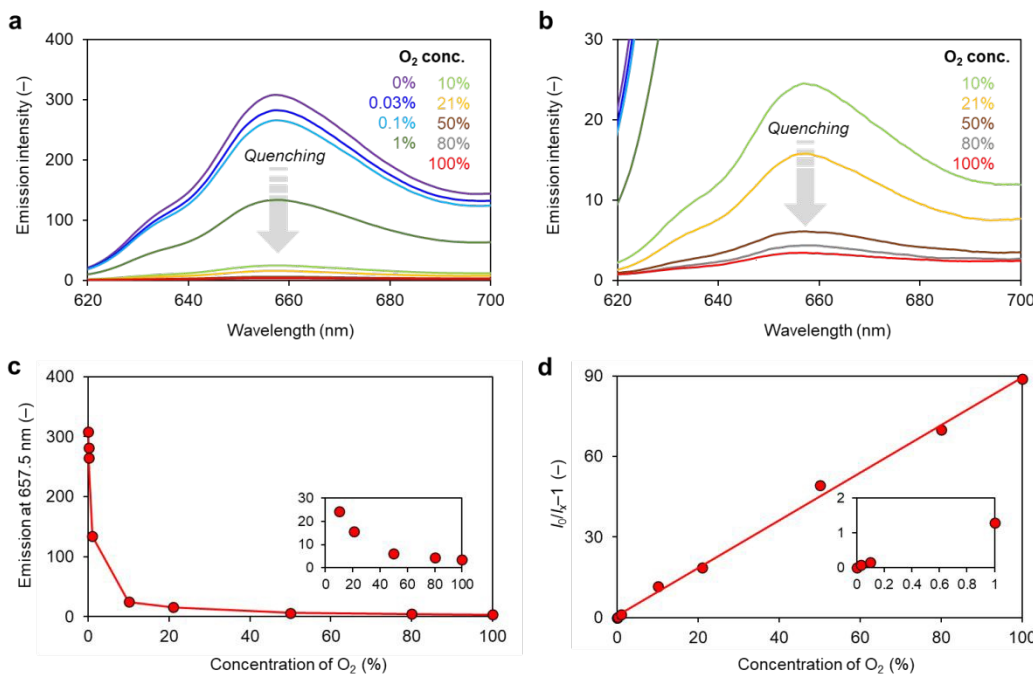


Figure 3. (a, b) Emission spectra of a neat film **PtPL** ($\lambda_{\text{ex}} = 412$ nm) measured under various O₂ concentrations (a; with higher emission intensities, b; emission intensities lower than 30). See **Figure S10** for photographs illustrating the emission changes of neat **PtPL** films at different O₂ levels. (c) Plot of O₂ concentration vs. emission intensity ($\lambda_{\text{em}} = 657.5$ nm) in a neat film **PtPL**. Inset shows intensities lower than 30. (d) Stern-Volmer plot of a neat film **PtPL** ($\lambda_{\text{em}} = 657.5$ nm) for O₂ sensing. Inset shows the plot for lower O₂ concentration than 1%. It is worth noting that the phosphorescence of **PtPL** shows little sensitivity to humidity, whereas it is sensitive to temperature and air pressure (see **Figures S15-17**).

To investigate the effect of the bulky alkyl side chains compared to a porous polymer matrix, the O₂ sensing performance of the neat liquid **PtPL** was compared with **PtTPP-PTMSP** and **PtPL-PTMSP** composites. A solution of **PtTPP** and **PTMSP** was spin-coated on a quartz substrate, and the optical properties of the thin films were investigated (**Figure 4a**). Absorption signals corresponding to the Soret-band ($\lambda_{\text{max}} = 401$ nm) of **PtTPP** linearly increased when the amount of **PtTPP** was increased from 0.2 to 20 wt% (**Figure 4b**). However, the absorption signals did not grow beyond 20 wt%, suggesting aggregation or precipitation of **PtTPP** either within or outside the polymer matrix. In contrast, absorption signals of **PtPL** blended into **PTMSP** ($\lambda_{\text{max}} =$

406 nm) did not saturate even at 80 wt% owing to the absence of aggregation of **PtPL** in the **PtPL-PTMSP** composite (**Figure 4c**). Composite films of **PtTPP-PTMSP** (1, 5, 20, and 50 wt%) exhibited slightly better sensitivity to O₂ ($I_0/I_{100} = \sim 120$) than a neat liquid film of **PtPL** ($I_0/I_{100} = \sim 90$), which can be attributed to the higher gas permeability of **PTMSP** compared to **PtPL** (**Figure 4e**). The linearity of each plot was quantitatively assessed using the coefficient of determination (R^2) obtained from linear fitting, showing moderate linearity ($R^2 = 0.84\text{--}0.97$). In contrast, **PtPL-PTMSP** displays clear composition-dependent behavior (**Figure 4d**). At low loadings (1, 5, and 20 wt%), a nonlinear response with high sensitivity is observed. This high sensitivity can be attributed to the high gas permeability of the **PTMSP** matrix as well as the increased number of O₂ molecules available per **PtPL** molecule. Another possible interpretation is that **PtPL**, bearing branched alkyl chains reminiscent of those typically present in plasticizers, may slightly modify the local polymer environment, potentially facilitating O₂ diffusion. By contrast, at higher loadings (50 and 100 wt%), the Stern–Volmer plots exhibit excellent linearity ($R^2 > 0.99$), while maintaining a sufficiently high level of sensitivity compared with other materials, despite some reduction. Such excellent linearity is advantageous for the quantification of a wide O₂ range based on two-point calibration. Downward-curved Stern–Volmer plots are commonly observed in sensor films and are often attributed to the presence of multiple emissive states with different luminescence lifetimes and/or quenching efficiencies within heterogeneous matrices.^{27,53–56} Thus, the improvement of linearity is likely due to the increased homogeneity of the sensing phase upon reducing the influence of the polymer matrix, which suppresses microenvironmental heterogeneity. Although neat liquid **PtPL** shows the lowest sensitivity among the samples in **Figure 4d**, this limitation is addressed in the blended liquid system discussed in a later section, where both high sensitivity and good linearity are simultaneously achieved.

Notably, neat liquid **PtPL** shows better photostability than **PtTPP-PTMSP** upon repeated measurements, which can be ascribed to protecting the Pt(II)-porphyrin unit by the bulky alkyl chains (**Figure 4f**). Although fluorinated porphyrins are known to show improved photostability,⁵⁷ fluorinated organic compounds potentially cause environmental concerns due to poor biodegradability. The core-shielding effect of phosphorescent liquids (*e.g.*, **PtPL**) by hydrocarbon alkyl chains is advantageous in this regard. Toward practical implementation, photostability could be further improved by elongating or densifying the branched alkyl chains; however, this may adversely affect O₂ sensitivity because of reduced energy transfer efficiency. Therefore,



photostability and sensitivity should be balanced depending on the aim of the application. We note that the present study focused on the equilibrium response to O_2 , and response time was not evaluated due to the unavailability of appropriate equipment. Overall, these studies elucidated, for the first time, that phosphorescent solvent-free liquids can be a promising platform for creating advanced optical gas sensors with high dye-loading amounts, excellent sensitivity, linearity, and photostability.

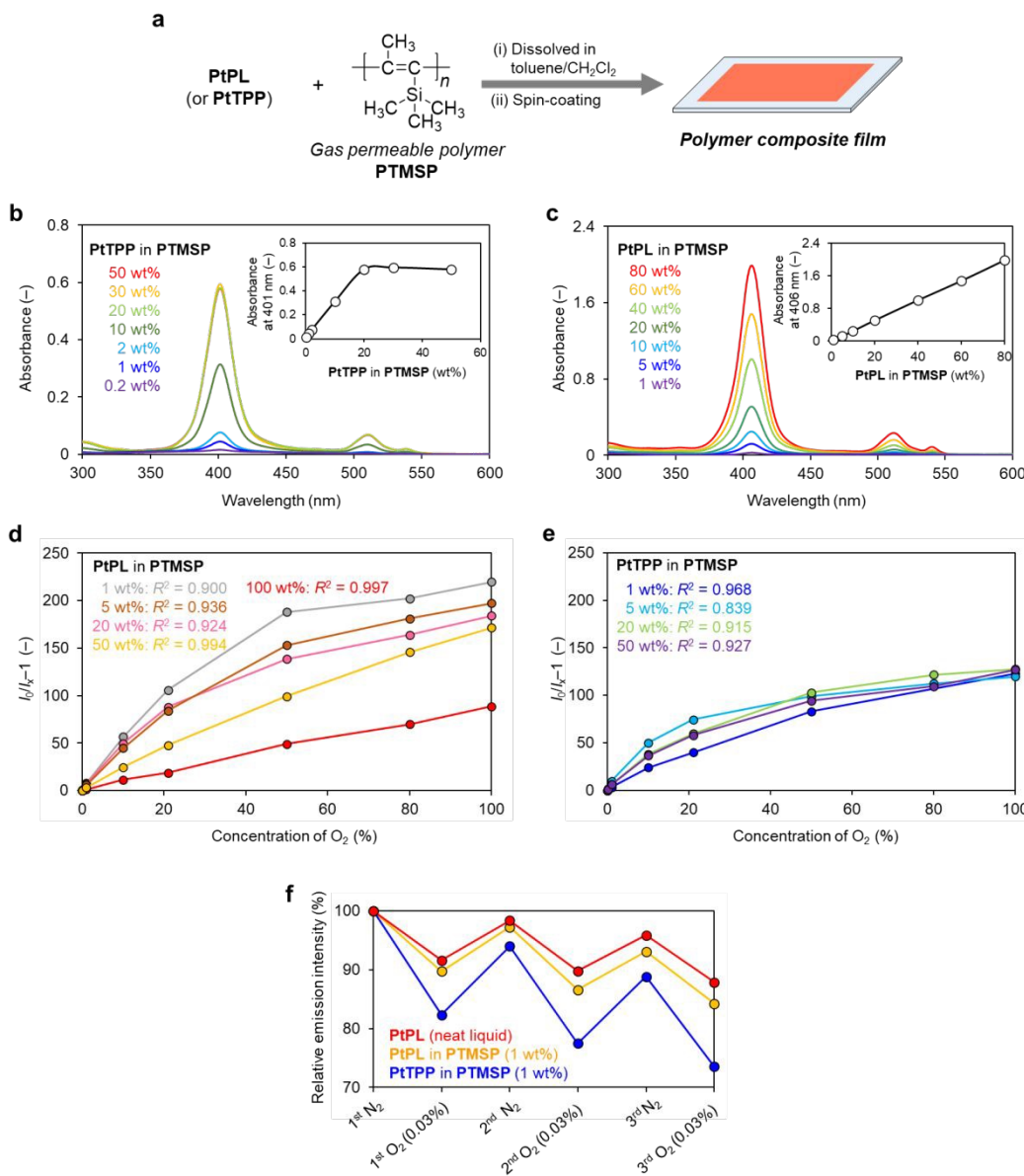


Figure 4. (a) Preparation of polymer composite films. (b) Absorption spectra of **PtTPP-PTMSP** composite film with various amounts of **PtTPP**. (c) Absorption spectra of **PtPL-PTMSP** composite film with various amounts of **PtPL**. (d) Stern-Volmer plots of neat liquid **PtPL** (100 wt%) and **PtPL-PTMSP** composite films (1, 5, 20, and 50 wt%). R^2 denotes the coefficient of determination for the linear fit. (e) Stern-Volmer plots of **PtTPP-PTMSP** composite films (1, 5, 20, and 50 wt%). (f) Decay of emission intensity upon repeated exposure to excited beam irradiations under N_2 and 0.03% O_2 .

Finally, ratiometric optical O_2 sensing was performed simply by blending **PtPL** with an alkylated pyrene fluorescent (O_2 -insensitive) liquid **PyL**⁵⁸ (**Figures 5a** and **S18**). The emission intensity of dye-loaded polymeric films can be influenced by various factors such as beam intensity, film thickness, and homogeneity of LOMs in the polymer matrix, and the accurate determination of I_0 (*i.e.*, emission intensity in the absence of O_2) is indispensable for reliable quantification of O_2 .^{24,27,59} To avoid frequent calibrations, ratiometric O_2 detection based on phosphorescent (O_2 sensitive) and fluorescent (O_2 insensitive) dyes is a promising approach.^{60–62} In the present study, ratiometric O_2 sensing was achieved simply by blending two types of liquids. Since both **PtPL** and **PyL** are hydrophobic and have similar liquid physical properties due to the same 2-hexyldecyl branched alkyl chains, the two liquids are miscible with each other,⁶³ and the blended liquid contains absorption profiles from both individual components (**Figure 5a,b**). Two films (A and B) with different loadings were prepared from the blended liquid of **PtPL+PyL** (1:2, by weight) and investigated for ratiometric O_2 sensing (**Figure 5c**). Upon excitation at 360 nm, the fluorescence ($\lambda_{em} = 428$ nm) from **PyL** is insensitive to O_2 , while the phosphorescence from **PtPL** ($\lambda_{em} = 656$ nm) is sensitive to O_2 . Stern-Volmer plots of the two films are highly linear ($R^2 > 0.999$), and the value of I_0/I_{100} in film A reaches ~ 120 (comparable to that of **PtTPP-PTMSP** in **Figure 4e**). A increase in O_2 sensitivity in the liquid blend system (compared with a neat liquid film of **PtPL**) may originate from enhanced O_2 solubility and/or diffusion in the liquid upon blending with the relatively smaller-sized molecule **PyL**. Stern-Volmer plots of films A and B are slightly different, presumably due to differences in the loading amount of liquid or experimental errors. Nevertheless, when ratios of phosphorescence and fluorescence are plotted against O_2 levels, films A and B



demonstrate almost identical linear lines despite nearly double the difference in their emission intensity. Thus, the miscibility of liquids offers reliable ratiometric O_2 sensing without the need for elaborate synthesis, fine-tuning of film loading, and frequent calibrations.

To confirm the enhanced sensitivity in the blended system, the sensitivity (I_0/I_{100}) of six independently prepared **PtPL** and **PtPL+PyL** films was statistically analyzed (**Tables S2 and S3**). As a result, the average sensitivity of **PtPL+PyL** ($I_0/I_{100} = 113.2, \sigma = 3.3$) was reproducibly higher than that of **PtPL** ($I_0/I_{100} = 75.3, \sigma = 1.8$). The sensitivity of **PtPL** in **Figure 3d** ($I_0/I_{100} \approx 90$) is slightly higher than that shown in Table S2 ($I_0/I_{100} = 75.3$ on average). This moderate difference can be attributed to cumulative decay of the emission intensity upon repeated exposure to excitation light (see **Figure 4f**). The data in **Figure 3** were obtained at multiple O_2 levels, with 100% O_2 measured at the final stage of the experiment, which likely led to a reduction in the I_{100} value compared to its actual value. In contrast, the data in **Table S2** were obtained from only two measurements, namely under N_2 for I_0 and under O_2 for I_{100} . Therefore, the values reported in **Table S2** are considered to be more reliable.



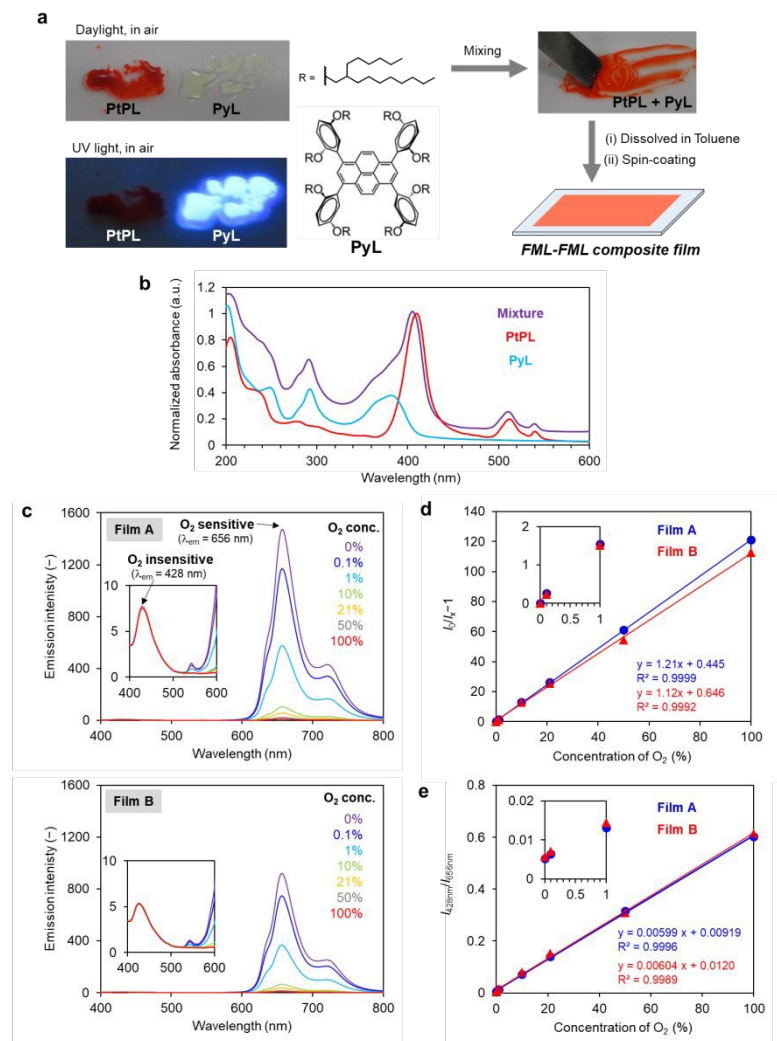


Figure 5. (a) Blending of phosphorescent liquid **PtPL** and fluorescent liquid **PyL**. (b) Absorption spectrum of the mixed liquid film of **PtPL+PyL** (1:2, by weight) measured in air. For comparison, the absorption spectra of the individual neat liquids (**PtPL** and **PyL**), measured separately, are also shown. (c) Emission spectra ($\lambda_{\text{ex}} = 360$ nm) of the mixed liquid film of **PtPL+PyL** (1:2, by weight) under various O_2 levels. The excitation wavelength was selected to simultaneously excite both **PtPL** and **PyL** while minimizing photobleaching caused by shorter-wavelength UV irradiation. Based on emission intensity, film A has approximately double the loading of liquids compared to film B. (d) Stern-Volmer plots obtained from phosphorescence ($\lambda_{\text{em}} = 656$ nm) of films A and B. (e) Ratiometric plots obtained from O_2 -insensitive fluorescence ($\lambda_{\text{em}} = 428$ nm) and O_2 -sensitive phosphorescence ($\lambda_{\text{em}} = 656$ nm) of films A and B.



Conclusions

This work reveals numerous benefits of luminescent core-isolated solvent-free liquids for optical gas sensing applications. Due to the liquid characteristics (*e.g.*, homogeneity, gas solubility, diffusion, and miscibility) and the shielding effects of the phosphorescent-core units by the bulky yet flexible alkyl chains, the Pt(II) porphyrin liquid demonstrates exceptional sensitivity, linearity, photostability, and calibration-free ratiometric operations in phosphorescent O₂ sensing. The concept presented in this study is broadly applicable to other functional π -chromophores and gaseous species, paving the way for a new platform for optical sensing materials.

Methods

Synthesis of PtPL. A previously reported liquid free-base porphyrin¹³ was used to prepare a liquid Pt(II) porphyrin (**PtPL**). Typically, the alkylated free-base porphyrin (140 mg, 0.055 mmol) and Pt(II)Cl₂ were refluxed in dry benzonitrile (15 ml) under an Ar atmosphere,⁵¹ and the progress of metalation was monitored by thin-layer chromatography (TLC) and variation in the Q-bands in the UV-Vis spectrum. After the reaction (ca. 4-5 h) was completed, the solvent was removed under reduced pressure, and the crude product was purified by column chromatography on silica gel (eluent: 10-20% CH₂Cl₂ in *n*-hexane). After drying under vacuum at 40 °C, a red-orange liquid (**PtPL**) was obtained (Yield: 80%). ¹H NMR (400 MHz, CDCl₃) in ppm: 8.86 (s, 8H, pyrrole β -H), 7.29 (d, *J* = 2.4 Hz, 8H, Ar-H), 6.86 (t, *J* = 2.0 Hz, 4H, Ar-H), 3.96 (d, *J* = 5.6 Hz, 16H, OCH₂), 1.83 (m, 8H, CH), 1.35-1.23 (m, 192H, CH₂), 0.82 (m, 48H, CH₃). ¹³C NMR (100 MHz, CDCl₃) in ppm: 158.68, 143.04, 140.62, 130.64, 122.18, 113.44, 101.21, 71.27, 38.10, 31.89, 31.86, 31.42, 30.03, 29.71, 29.59, 29.33, 26.87, 22.66, 14.11. HR-ESI-MS (m/z): calculated for [C₁₇₂H₂₈₅O₈N₄¹⁹⁴Pt]⁺ = 2729.1639 m/z, found 2729.1736 m/z.

Preparation of liquid films. Liquid films for O₂ sensing were obtained by spin-coating a toluene solution of liquid materials onto a quartz substrate. Typically, it took 5 seconds to reach 3000 rpm, and the film was dried at 3000 rpm for 60 seconds. Thus, homogeneous liquid films were obtained. The loading amount of the liquid film was adjusted by changing the concentration of the toluene solution or repeating the spin-coating process. A blended liquid film of **PtPL+PyL** was prepared from a solution of **PtPL** and **PyL** in toluene (1:2, by weight). Liquid films were dried in air for



more than 12 h before spectroscopic measurements. See **Figure S20** for a discussion of residual solvent in a liquid film.

Preparation of polymer films. Stock solutions of **PtPL** in dichloromethane (5.00 mg/ml) and **PTMSP**^{49,64} in toluene (10.0 mg/ml) were mixed at various ratios. The mixed solutions were spin-coated on a quartz substrate, as described above. In the case of **PtTPP**, a more diluted stock solution (1.67 mg/ml) in dichloromethane was used due to limited solubility. See **Figure S19** for a discussion on the homogeneity of **PtPL** in polymer films.

O₂ sensing. The porphyrin film containing quartz substrate was placed in a quartz cell (1 cm × 1 cm), as illustrated in **Figure S1**. The quartz cell was capped with a rubber septum, and then dry N₂ or Ar containing various concentrations of O₂ was flowed through the cell using inlet and outlet needles to measure emission spectra (FP-8300 spectrophotometer, JASCO) under controlled O₂ levels. The typical flow rate was 100 ml/min, and 5 min flow was sufficient to replace the interior gases of the small cell (~ 3 ml). The flow rate was adjusted and monitored using a float-ball-type flow meter (KOFLOCK) and a digital flow meter (7000 Flowmeter, Ellutia). Dry N₂ and O₂ from laboratory lines were used as 0% and 100% O₂, respectively. Ambient air supplied by a battery-powered pump (GSP-400FT, GASTEC) was regarded as 21% O₂. For 0.1%, 1%, and 10% O₂, standard gases supplied from high-pressure gas cylinders were directly used. For 50% and 80% O₂, dry N₂ and O₂ from laboratory lines were mixed at appropriate flow rates (monitored by digital flow meters). Similarly, 0.1% O₂ with dry N₂ dilution yielded 0.03% O₂.

Funding: This work was supported by JSPS KAKENHI (JP18H03922, JP24H01733, JP25H01264).

Data Availability Statement: The data presented in this study are available upon reasonable request from the corresponding authors.

Author Contributions. A.G. and T.M. synthesized porphyrins. A.G., S.I., and T.M. performed sensing experiments. M.K.C. and D.T.P. conducted material characterization. A.S. measured transient emission properties. T.H. provided PTMSP and discussed the results of O₂ sensing. S.I. wrote the manuscript with input from all other authors. All authors read and approved the final version of the manuscript. S.I. and T.N. designed and directed the research.



Acknowledgments: This work was supported by the World Premier International Research Center Initiative (WPI), MEXT, Japan. Ms. Reiko Takano is acknowledged for assisting with sensing measurements. Dr. Zhenfeng Guo and Mr. Mina Fahmy are acknowledged for supporting the spectroscopic measurements.

Conflicts of Interest: The authors declare no conflicts of interest.

Supporting Information: Supporting Information is available from online.

References

- (1) *Functional Organic Liquids* (Ed.: T. Nakanishi), Wiley-VCH, Weinheim 2019.
- (2) A. Ghosh and T. Nakanishi, Frontiers of Solvent-Free Functional Molecular Liquids, *Chem. Commun.*, 2017, **53**, 10344–10357.
- (3) F. Lu and T. Nakanishi, Solvent-Free Luminous Molecular Liquids, *Adv. Optical Mater.*, 2019, **7**, 1900176.
- (4) A. Tateyama and T. Nakanishi, Responsive Molecular Liquid Materials, *Responsive Mater.*, 2023, **1**, e20230001.
- (5) S. S. Babu, J. Aimi, H. Ozawa, N. Shirahata, A. Saeki, S. Seki, A. Ajayaghosh, H. Möhwald and T. Nakanishi, Solvent-Free Luminescent Organic Liquids, *Angew. Chem. Int. Ed.*, 2012, **51**, 3391–3395.
- (6) Goudappagouda, A. Manthanath, V. C. Wakchaure, K. C. Ranjeesh, T. Das, K. Vanka, T. Nakanishi and S. S. Babu, Paintable Room Temperature Phosphorescent Liquid Formulations of Alkylated Bromonaphthalimide, *Angew. Chem. Int. Ed.*, 2019, **58**, 2284–2288.
- (7) M. Komura, T. Ogawa and Y. Tani, Room-Temperature Phosphorescence of a Supercooled Liquid: Kinetic Stabilisation by Desymmetrisation, *Chem. Sci.*, 2021, **12**, 14363–14368.
- (8) A. Ikenaga, Y. Akiyama, T. Ishiyama, M. Gon, K. Tanaka, Y. Chujo and K. Isoda, Stimuli-Responsive Self-Assembly of π -Conjugated Liquids Triggers Circularly Polarized Luminescence, *ACS Appl. Mater. Interfaces*, 2021, **13**, 47127–47133.
- (9) Y. Tani, Y. Oshima, R. Okada, J. Fujimura, Y. Miyazaki, M. Nakano, O. Urakawa, T. Inoue, T. Ehara, K. Miyata, K. Onda and T. Ogawa, Fast and Efficient Room-Temperature



Phosphorescence from Metal-Free Organic Molecular Liquids, *Chem. Sci.*, 2025, **16**, 17480–17486.

(10) P. Duan, N. Yanai and N. Kimizuka, Photon Upconverting Liquids: Matrix-Free Molecular Upconversion Systems Functioning in Air, *J. Am. Chem. Soc.*, 2013, **135**, 19056–19059.

(11) R. K. Gupta, T. Nakanishi and D. T. Payne, Alkyl- π Liquids as Condensed-State Singlet Oxygen Photosensitizers, *Chem. Eur. J.*, 2025, **31**, e202500739.

(12) S. Hirata, K. Kubota, H. H. Jung, O. Hirata, K. Goushi, M. Yahiro and C. Adachi, Improvement of Electroluminescence Performance of Organic Light-Emitting Diodes with a Liquid-Emitting Layer by Introduction of Electrolyte and a Hole-Blocking Layer, *Adv. Mater.*, 2011, **23**, 889–893.

(13) A. Ghosh, M. Yoshida, K. Suemori, H. Isago, N. Kobayashi, Y. Mizutani, Y. Kurashige, I. Kawamura, M. Nirei, O. Yamamuro, T. Takaya, K. Iwata, A. Saeki, K. Nagura, S. Ishihara and T. Nakanishi, Soft Chromophore Featured Liquid Porphyrins and their Utilization toward Liquid Electret Applications, *Nat. Commun.*, 2019, **10**, 4210.

(14) Y. Shi, M. A. Gerkman, Q. Qiu, S. Zhang and G. D. D. Han, Sunlight-Activated Phase Change Materials for Controlled Heat Storage and Triggered Release, *J. Mater. Chem. A*, 2021, **9**, 9798–9808.

(15) N. Giri, M. G. Del Pópolo, G. Melaugh, R. L. Greenaway, K. Rätzke, T. Koschine, L. Pison, M. F. Costa Gomes, A. I. Cooper and S. L. James, Liquids with Permanent Porosity, *Nature*, 2015, **527**, 216–220.

(16) Y.-H. Zou, Y.-B. Huang, D.-H. Si, Q. Yin, Q.-J. Wu, Z. Weng and R. Cao, Porous Metal–Organic Framework Liquids for Enhanced CO₂ Adsorption and Catalytic Conversion, *Angew. Chem. Int. Ed.*, 2021, **60**, 20915–20920.

(17) M. J. Hollamby, M. Karny, P. H. H. Bomans, N. A. J. M. Sommerdijk, A. Saeki, S. Seki, H. Minamikawa, I. Grillo, B. R. Pauw, P. Brown, J. Eastoe, H. Möhwald and T. Nakanishi, Directed Assembly of Optoelectronically Active Alkyl- π -Conjugated Molecules by Adding n-Alkanes or π -Conjugated Species, *Nat. Chem.*, 2014, **6**, 690–696.

(18) T. Ogoshi, K. Maruyama, Y. Sakatsume, T. Kakuta, T. Yamagishi, T. Ichikawa and M. Mizuno, Guest Vapor-Induced State Change of Structural Liquid Pillar[6]arene, *J. Am. Chem. Soc.*, 2019, **141**, 785–789.

(19) A. Shinohara, C. Pan, Z. Guo, L. Zhou, Z. Liu, L. Du, Z. Yan, F. J. Stadler, L. Wang and



Nakanishi, Viscoelastic Conjugated Polymer Fluids, *Angew. Chem. Int. Ed.*, 2019, **58**, 9581–9585.

(20) K. Isoda, M. Matsubara, A. Ikenaga, Y. Akiyama and Y. Mutoh, Reversibly/Irreversibly Stimuli-Responsive Inks Based on N-Heteroacene Liquids, *J. Mater. Chem. C*, 2019, **7**, 14075–14079.

(21) K. Isoda, T. Ishiyama, Y. Mutoh and D. Matsukuma, Stimuli-Responsive Room-Temperature N-Heteroacene Liquid: In Situ Observation of the Self-Assembling Process and Its Multiple Properties, *ACS Appl. Mater. Interfaces*, 2019, **11**, 12053–12062.

(22) 'Henry's law' in IUPAC Compendium of Chemical Terminology, 5th ed. International Union of Pure and Applied Chemistry; 2025. Online version 5.0.0, 2025. <https://doi.org/10.1351/goldbook.H02783>.

(23) O. S. Wolfbeis, Materials for Fluorescence-Based Optical Chemical Sensors, *J. Mater. Chem.*, 2005, **15**, 2657–2669.

(24) C. McDonagh, C. S. Burke and B. D. MacCraith, Optical Chemical Sensors, *Chem. Rev.*, 2008, **108**, 400–422.

(25) S. W. Thomas, G. D. Joly and T. M. Swager, Chemical Sensors Based on Amplifying Fluorescent Conjugated Polymers, *Chem. Rev.*, 2007, **107**, 1339–1386.

(26) J. Kramer, R. Kang, L. M. Grimm, L. De Cola, P. Picchetti and F. Biedermann, Molecular Probes, Chemosensors, and Nanosensors for Optical Detection of Biorelevant Molecules and Ions in Aqueous Media and Biofluids, *Chem. Rev.*, 2022, **122**, 3459–3636.

(27) X.-D. Wang and O. S. Wolfbeis, Optical Methods for Sensing and Imaging Oxygen: Materials, Spectroscopies and Applications, *Chem. Soc. Rev.*, 2014, **43**, 3666–3761.

(28) R. Ramamoorthy, P. K. Dutta and S. A. Akbar, Oxygen Sensors: Materials, Methods, Designs and Applications, *J. Mater. Sci.*, 2003, **38**, 4271–4282.

(29) A. A. Mendonsa and K. J. Cash, Oxygen-Sensitive Optical Nanosensors: Current Advances and Future Perspectives, *ACS Sens.*, 2025, **10**, 3194–3206.

(30) J. W. Gregory, H. Sakaue, T. Liu and J. P. Sullivan, Fast Pressure-Sensitive Paint for Flow and Acoustic Diagnostics, *Annu. Rev. Fluid Mech.*, 2014, **46**, 303–330.

(31) J. Inukai, K. Miyatake, K. Takada, M. Watanabe, T. Hyakutake, H. Nishide, Y. Nagumo, M. Watanabe, M. Aoki and H. Takano, Direct Visualization of Oxygen Distribution in Operating Fuel Cells, *Angew. Chem. Int. Ed.*, 2008, **47**, 2792–2795.

(32) Y. E. Koo Lee, E. E. Ulbrich, G. Kim, H. Hah, C. Strollo, W. Fan, R. Gurjar, S. Koo and R.



Kopelman, Near Infrared Luminescent Oxygen Nanosensors with Nanoparticle Matrix Tailored Sensitivity, *Anal. Chem.*, 2010, **82**, 8446–8455.

(33) X. Zheng, H. Mao, D. Huo, W. Wu, B. Liu and X. Jiang, Successively Activatable Ultrasensitive Probe for Imaging Tumour Acidity and Hypoxia, *Nat. Biomed. Eng.*, 2017, **1**, 0057.

(34) J. Mei, N. L. C. Leung, R. T. K. Kwok, J. W. Y. Lam, and B. Z. Tang, Aggregation-Induced Emission: Together We Shine, United We Soar!, *Chem. Rev.*, 2015, **115**, 11718–11940.

(35) Y. Amao, Probes and Polymers for Optical Sensing of Oxygen, *Microchim. Acta*, 2003, **143**, 1–12.

(36) S. M. Borisov, A. S. Vasylevska, C. Krause and O. S. Wolfbeis, Composite Luminescent Material for Dual Sensing of Oxygen and Temperature, *Adv. Funct. Mater.*, 2006, **16**, 1536–1542.

(37) H. Xiang, L. Zhou, Y. Feng, J. Cheng, D. Wu and X. Zhou, Tunable Fluorescent/Phosphorescent Platinum(II) Porphyrin–Fluorene Copolymers for Ratiometric Dual Emissive Oxygen Sensing, *Inorg. Chem.*, 2012, **51**, 5208–5212.

(38) S.-K. Lee and I. Okura, Porphyrin-Doped Sol-Gel Glass as a Probe for Oxygen Sensing, *Anal. Chim. Acta*, 1997, **342**, 181–188.

(39) S. M. Borisov, P. Lehner and I. Klimant, Novel Optical Trace Oxygen Sensors Based on Platinum(II) and Palladium(II) Complexes with 5,10,15,20-meso-Tetrakis-(2,3,4,5,6-pentafluorophenyl)-porphyrin Covalently Immobilized on Silica-Gel Particles, *Anal. Chim. Acta*, 2011, **690**, 108–115.

(40) C.-S. Chu and Y.-L. Lo, High-performance Fiber-Optic Oxygen Sensors Based on Fluorinated Xerogels Doped with Pt(II) Complexes, *Sens. Actuators B: Chem.*, 2007, **124**, 376–382.

(41) B.-H. Han, I. Manners and M. A. Winnik, Oxygen Sensors Based on Mesoporous Silica Particles on Layer-by-Layer Self-Assembled Films, *Chem. Mater.*, 2005, **17**, 3160–3171.

(42) T. Burger, C. Winkler, I. Dalfen, C. Slugovc and S. M. Borisov, Porphyrin based Metal–Organic Frameworks: Highly Sensitive Materials for Optical Sensing of Oxygen in Gas Phase, *J. Mater. Chem. C*, 2021, **9**, 17099–17112.

(43) Y. E. Koo, Y. Cao, R. Kopelman, S. M. Koo, M. Brasuel and M. A. Philbert, Real-Time Measurements of Dissolved Oxygen Inside Live Cells by Organically Modified Silicate Fluorescent Nanosensors, *Anal. Chem.*, 2004, **76**, 2498–2505.

(44) X.-D. Wang, J. A. Stolwijk, T. Lang, M. Sperber, R. J. Meier, J. Wegener and O. S. Wolfbeis, Ultra-Small, Highly Stable, and Sensitive Dual Nanosensors for Imaging Intracellular Oxygen and



pH in Cytosol, *J. Am. Chem. Soc.*, 2012, **134**, 17011–17014.

(45) C. M. Lemon, E. Karnas, M. G. Bawendi and D. G. Nocera, Two-Photon Oxygen Sensing with Quantum Dot-Porphyrin Conjugates, *Inorg. Chem.*, 2013, **52**, 10394–10406.

(46) Y. Amao and I. Okura, Optical Oxygen Sensor Devices Using Metalloporphyrins, *J. Porphyrins Phthalocyanines*, 2009, **13**, 1111–1122.

(47) I. Okura and T. Kamachi, Applications of Porphyrins and Related Compounds as Optical Oxygen Sensors, In *Handbook of Porphyrin Science*; K. M. Kadish, K. M. Smith and R. Guilard, Eds.; World Scientific Publishing: Singapore, 2011, **12**, 297–348.

(48) S. Ishihara, J. Labuta, W. V. Rossom, D. Ishikawa, K. Minami, J. P. Hill and K. Ariga, Porphyrin-Based Sensor Nanoarchitectonics in Diverse Physical Detection Modes, *Phys. Chem. Chem. Phys.*, 2014, **16**, 9713–9746.

(49) T. Masuda, E. Isobe, T. Higashimura and K. Takada, Poly[1-(trimethylsilyl)-1-propyne]: A New High Polymer Synthesized with Transition-Metal Catalysts and Characterized by Extremely High Gas Permeability, *J. Am. Chem. Soc.*, 1983, **105**, 7473–7474.

(50) Y. Amao, K. Asai, I. Okura, H. Shinohara and H. Nishide, Platinum Porphyrin Embedded in Poly(1-trimethylsilyl-1-propyne) Film as an Optical Sensor for Trace Analysis of Oxygen, *Analyst*, 2000, **125**, 1911–1914.

(51) W. Wu, W. Wu, S. Ji, H. Guo, X. Wang and J. Zhao, The Synthesis of 5, 10, 15, 20-Tetraarylporphyrins and their Platinum (II) Complexes as Luminescent Oxygen Sensing Materials, *Dyes Pigm.*, 2011, **89**, 199–211.

(52) A. Gugliuzza, A. Iulianelli and A. Basile, Membranes for Hydrocarbon Fuel Processing and Separation. In *Advanced Membrane Science and Technology for Sustainable Energy and Environmental Applications*; Elsevier, 2011, 295–338.

(53) E. R. Caraway, J. N. Demas, B. A. DeGraff and J. R. Bacon, Photophysics and Photochemistry of Oxygen Sensors Based on Luminescent Transition-Metal Complexes, *Anal. Chem.*, 1991, **63**, 337–342.

(54) J. N. Demas, B. A. DeGraff and W. Xu, Modeling of Luminescence Quenching-Based Sensors: Comparison of Multisite and Nonlinear Gas Solubility Models, *Anal. Chem.*, 1995, **67**, 1377–1380.

(55) P. Hartmann, M. J. P. Leiner and M. E. Lippitsch, Luminescence Quenching Behavior of an Oxygen Sensor Based on a Ru(II) Complex Dissolved in Polystyrene, *Anal. Chem.*, 1995, **67**, 88–



93.

(56) W. Xu, R. C. McDonough, B. Langsdorf, J. N. Demas and B. A. DeGraff, Oxygen Sensors Based on Luminescence Quenching: Interactions of Metal Complexes with the Polymer Supports, *Anal. Chem.*, 1994, **66**, 4133–4141.

(57) W. W. S. Lee, K. Y. Wong, X. M. Li, Y. B. Leung, C. S. Chan and K. S. Chan, Halogenated Platinum Porphyrins as Sensing Materials for Luminescence-Based Oxygen Sensors, *J. Mater. Chem.*, 1993, **3**, 1031–1035.

(58) F. Lu, T. Takaya, K. Iwata, I. Kawamura, A. Saeki, M. Ishii, K. Nagura and T. Nakanishi, A Guide to Design Functional Molecular Liquids with Tailorable Properties using Pyrene-Fluorescence as a Probe, *Sci. Rep.*, 2017, **7**, 3416.

(59) P. Lehner, C. Staudinger, S. M. Borisov, J. Regensburger and I. Klimant, Intrinsic Artifacts in Optical Oxygen Sensors—How Reliable are our Measurements?, *Chem. Eur. J.*, 2015, **21**, 3978–3986.

(60) Y. Feng, J. Cheng, L. Zhou, X. Zhou and H. Xiang, Ratiometric Optical Oxygen Sensing: A Review in Respect of Material Design, *Analyst*, 2012, **137**, 4885–4901.

(61) T. Hyakutake, I. Okura, K. Asai and H. Nishide, Dual-Mode Oxygen-Sensing Based on Oxygen-Adduct Formation at Cobaltporphyrin–Polymer and Luminescence Quenching of Pyrene: An Optical Oxygen Sensor for a Practical Atmospheric Pressure, *J. Mater. Chem.*, 2008, **18**, 917–922.

(62) H. Zhao, L. Zang, L. Wang, F. Qin, Z. Zhang and W. Cao, Luminescence Ratiometric Oxygen Sensor Based on Gadolinium Labeled Porphyrin and Filter Paper, *Sens. Actuators B*, 2015, **215**, 405–411.

(63) Z. Guo, C. Pan, A. Shinohara and T. Nakanishi, Merging π -Molecular Functions Achieved through Homogeneous Liquid-Liquid Blending of Solvent-Free Alkyl- π Liquids, *Sci. Tech. Adv. Mater.*, 2025, **26**, 2515007.

(64) W. Waskitoaji, T. Hyakutake, J. Kato, M. Watanabe and H. Nishide, Biplanar Visualization of Oxygen Pressure by Sensory Coatings of Luminescent Pt-Porpholactone and -Porphyrin Polymers, *Chem. Lett.*, 2009, **38**, 1164–1165.



Data Availability Statement: The data presented in this study are available upon reasonable request from the corresponding authors.